Propagating Elementary Excitation in a Dilute Optical Lattice

J.-Y. Courtois,* S. Guibal, D. R. Meacher,† P. Verkerk, and G. Grynberg

Laboratoire Kastler-Brossel, Département de Physique de l'Ecole Normale Supérieure, 24, rue Lhomond, F-75231 Paris cedex 05, France

(Received 28 February 1996)

Propagating elementary excitations characterized by a well-defined propagation velocity (such as acoustic waves) are usually considered as being typical of condensed matter or dense fluids. We show that this requirement is actually not necessary. We predict in the case of a dilute optical lattice the occurrence of a propagating excitation mode which can induce a stimulated scattering mechanism analogous to stimulated Brillouin scattering, although it does not involve any interaction between atoms. We also present the results of an experimental investigation in cesium that demonstrates the existence of this novel stimulated scattering process. [S0031-9007(96)00554-6]

PACS numbers: 32.80.Pj, 32.60.+i

The dynamical properties of a material medium can be formally characterized by the ensemble of its elementary excitation modes and their associated eigenfrequencies. When investigated through fluorescence, intensity correlation, or pump-probe spectroscopy, such dynamical eigenmodes manifest themselves in the form of resonances having a width and position related to the real and imaginary parts of their eigenfrequencies, respectively. It is traditional to distinguish between three regions of the spectra associated with excitation modes corresponding to pure damping processes, spatially localized oscillations, or spatially delocalized propagating excitations, respectively [1]. The former, which is associated with Rayleigh scattering, includes all the central features of the spectrum. These Rayleigh resonances are essentially characterized by the damping rates of the relevant excitation modes. The second region comprises sideband Raman resonances arising from transitions between nondegenerate and differently populated energy levels of the scattering particles. The main characteristic of Raman scattering is the oscillation frequency of the excitation, which determines the position of the Raman resonances, no matter the details of the experimental geometry. By contrast, the third region of the spectrum is associated with resonant light scattering from propagating excitation waves, the prototype of which is Brillouin scattering. The positions of the associated sideband resonances depend on the details of the experimental geometry through a dispersion relation involving the propagation velocity of the delocalized excitation, which is the main feature of such resonances. To date, propagating elementary excitations have been only reported in condensed matter or dense fluids, where particle interactions are sufficiently strong to support acoustic or spin wave propagation. We show in this paper that this requirement is actually not necessary for propagating excitation to take place in a medium. More precisely, we predict in the case of a dilute optical lattice [2] consisting of a periodic structure of micron-sized potential wells induced by the light shift of the atomic sublevels in a standing wave, the occurrence of a propagating excitation mode consisting of repeated cycles of half oscillations in a potential well followed by optical pumping toward an adjacent potential well. We show that the associated propagating density modulation can induce a stimulated scattering process, and we present the results of an experimental investigation that actually demonstrates its occurrence.

We consider a standard four beam optical lattice [3] consisting of two x-polarized beams propagating in the yOz plane and making an angle $2\theta_y$, and two y-polarized beams propagating in the xOz plane and making an angle $2\theta_x$. As shown previously [4], this configuration is well suited for Sisyphus cooling, so in steady state most of the atoms are localized at the bottom of the optical potential wells, where they undergo an oscillatory motion characterized by the oscillation frequencies $\Omega_{x,y,z}$ along the three directions Ox, y, z, respectively. The variation of the optical potential along an x axis connecting the potential minima is shown in Fig. 1(a) for the simple case of a $J = 1/2 \rightarrow J' = 3/2$ atomic transition. Note that the light polarization at the bottom of the optical potential wells is alternatively σ^+ and σ^-, and that the distance between two adjacent wells is $\lambda_x/2 = \lambda/2 \sin\theta_x \approx \lambda/2\theta_x$ in the small angle limit considered here (λ is the wavelength of the lattice beams). In fact, even though most of the atoms are bound inside a well, a few delocalized atoms still propagate over this periodic structure. Semiclassical Monte Carlo simulations of the atomic motion [5] show that the dominant propagation mode along the x direction for such atoms consists of the following steps: (i) half oscillation in a σ^- potential well (the atom moves from A to B), (ii) optical pumping from a σ^- to a σ^+ potential curve (the atomic velocity is almost unchanged by the photon recoil), (iii) half oscillation in a σ^+ potential well (the atom moves from B to C), (iv) optical pumping from a σ^+ to a σ^- potential curve, (v) half oscillation in a σ^- potential well (the atom moves from C to D), and so on. We show in Fig. 1(b) a typical example of computed trajectory [6] where a previously localized atom travels over

 0031-9007/96/77(1)/40(4)$10.00

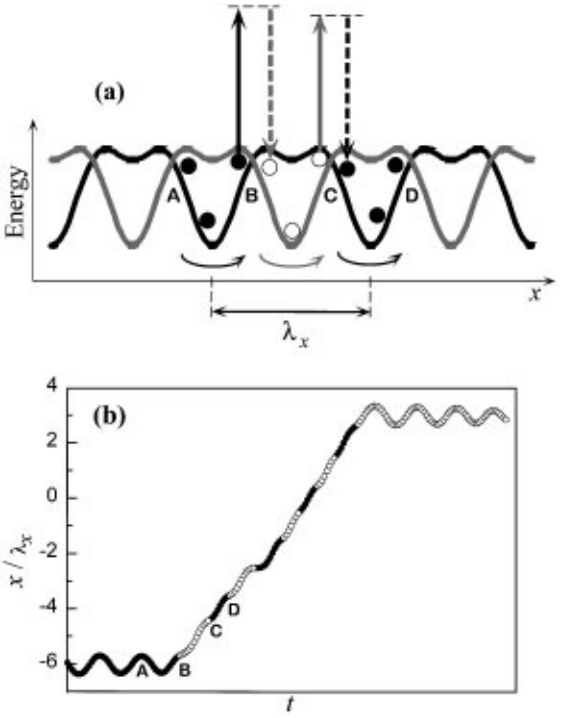

FIG. 1. (a) Section of the optical bipotential of a $J = 1/2 \rightarrow J' = 3/2$ standard optical lattice along the direction $y = z = 0$. An atom can propagate along this periodic structure through a sequence of half oscillations in a well (such as AB, BC, etc.) followed by transitions toward adjacent wells due to optical pumping. (b) Example of trajectory followed by an atom: the atom is in the $m = -1/2$ ($m = +1/2$) state when the dot is black (empty).

eight potential wells through this half oscillation-optical pumping sequence before being trapped back in a well. [This propagation mode is in strong contrast with the one taking place in the conventional one-dimensional lin⊥lin optical lattice [7]. This is because in the present polarization configuration, transitions between the $m = -1/2$ and $m = +1/2$ states are strongly suppressed near the bottom x_w of a potential well because of the local intensity of the minority circular polarization component's varying as $(x - x_w)^4$ [3].] If one neglects the influence of the potential anharmonicity, an atom travels from A to B, B to C, or C to D in a typical time τ equal to half the oscillation period in a well, namely, $\tau = \pi/\Omega_x$. Elementary propagating excitations taking the form of density waves are therefore expected to propagate at the average velocity $\overline{v} = \lambda_x/2\tau = \lambda\,\Omega_x/2\pi\theta_x$. Under appropriate conditions, such density modulations can be driven by the modulation of the optical potential and of the optical pumping rate induced by a pump-probe interference pattern, provided that its phase velocity along the x direction be equal to $\pm\overline{v}$. More quantitatively, denoting by $\mathbf{k}_p$ and $\omega_p = \omega + \delta$ the wave vector and frequency of the probe beam, respectively, and by $\mathbf{k}$ and ω those of one pump (lattice) beam, the pump-probe interference pattern moves along Ox with the velocity $v = \delta/(\mathbf{k}_p - \mathbf{k}) \cdot \mathbf{e}_x$. In the situation where the probe beam makes a small angle θ_p with Oz and has the same linear polarization as the nearly copropagating beams, the two interference patterns associated with these two lattice beams are characterized by the phase velocities $v_\pm = \delta/k(\theta_p \pm \theta_x)$. The resonant driving condition $|v_\pm| = \overline{v}$ then yields $\delta = \pm\Omega_{S+}$ and $\delta = \pm\Omega_{S-}$ with

$$\Omega_{S\pm} = \Omega_x|\theta_p \pm \theta_x|/\theta_x\,. \tag{1}$$

In particular, when the probe is aligned along Oz ($\theta_p = 0°$), the resonance condition simplifies to $\delta = \pm\Omega_x$, which means that a resonant structure is expected at the position $\Omega_S = \Omega_x$ of the Ox vibration frequency. Furthermore, because in this geometry the excitation of the Ω_x vibration mode is forbidden for symmetry reasons [8], the existence of a resonance located around Ω_x on the probe transmission spectrum cannot originate from stimulated Raman scattering, and can thus be attributed to a novel stimulated scattering mechanism associated with the aforementioned propagating excitation. When $\theta_p \neq 0°$ two atomic density waves differing in wavelengths ($\lambda_\pm = \lambda_x\theta_x/|\theta_p \pm \theta_x|$) are involved in the lattice response to the pump-probe excitation, the lower frequency mode having a spatial period larger than λ_x. Because the half oscillation-optical pumping sequences are more likely to be interrupted as the propagation distance increases, large scale spatial modulations of the density are more heavily damped than small scale variations, so one expects the Ω_{S-} resonance to have an amplitude smaller than the Ω_{S+} resonance.

In order to check the validity of this model, we performed numerical calculations of the probe transmission spectra using a semiclassical Monte Carlo simulation of the atomic dynamics. The principle of this simulation technique, which was applied in the case of a $J = 1/2 \rightarrow J' = 3/2$ transition by constraining the atomic motion in two dimensions, has been presented elsewhere [9]. Hereafter are summarized the essential results obtained for an atomic motion in the xOz plane. Figure 2 displays the probe transmission spectra calculated for $\theta_x = \theta_y = 20°$ and for two different angles of the probe $\theta_p = 0°$ (a) and $\theta_p = 10°$ (b). The resonances Ω_z and Ω_S are clearly visible on Fig. 2(a). By discriminating between the contributions of atoms having different mechanical energies, it is found that the center of the Ω_S line essentially arises from atoms having an energy larger than the optical bipotential crossing points. By contrast, the Ω_z resonance mainly involves bound atoms. Figure 2(b) ($\theta_p = 10°$) displays a probe spectrum with a large Ω_{S+} and a weak Ω_{S-} resonance shifted toward the high and low frequency domain compared to Ω_x, respectively, as expected from the preceding discussion. Furthermore, because the stimulated Raman resonance Ω_x is no longer forbidden with a probe tilted with respect to Oz, a supplementary structure appears between Ω_{S+} and Ω_{S-}.

We now present the results of an experimental investigation performed in cesium in order to demonstrate the

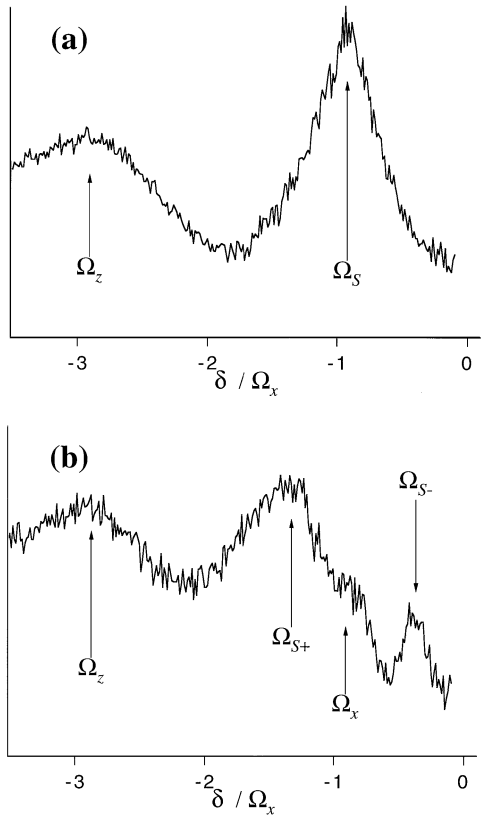

FIG. 2. Theoretical probe transmission spectra for $\theta_x = \theta_y = 20°$ and for two directions of the probe: $\theta_p = 0°$ (a) and $\theta_p = 10°$ (b). The probe has the same polarization as the nearly copropagating lattice beams.

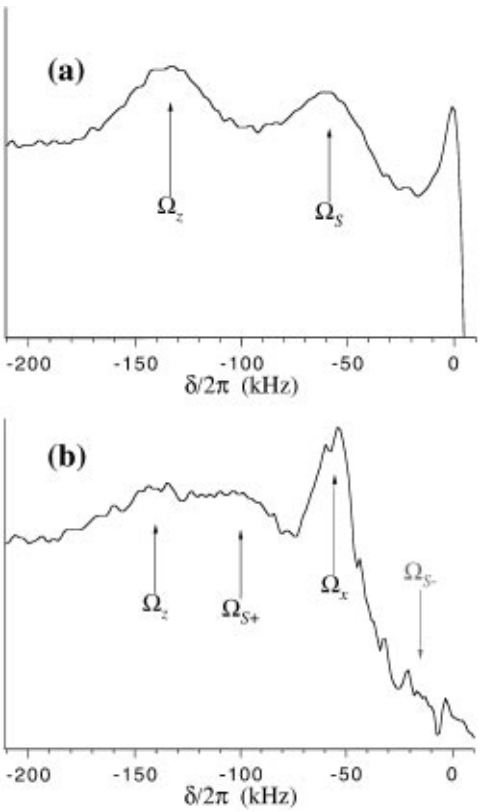

FIG. 3. Experimental probe transmission spectra for $\theta_x = \theta_y = 30°$ and for two directions of the probe: $\theta_p = 0°$ (a) and $\theta_p = 25°$ (b). The probe has the same polarization as the copropagating lattice beams. One can note that the width of the Ω_x vibrational line (b) is narrower than the width of the Ω_S resonance associated with the propagation mode (a). Note also that the propagation velocity of this mode, $\bar{v} \approx 10\ \mathrm{cm\,s^{-1}}$, is much larger than the recoil velocity $v_{\mathrm{rec}} \approx 0.35\ \mathrm{cm\,s^{-1}}$.

occurrence of the previously discussed propagating excitation mode. The experimental setup was described previously [4]. The lattice beams, whose intensity is typically 10 $\mathrm{mW/cm^2}$, are tuned on the red side of the $6S_{1/2}(F = 4) \rightarrow 6P_{3/2}(F' = 5)$ transition of cesium, the frequency detuning Δ being of the order of a few natural linewidths Γ. When a probe beam having the same polarization as the copropagating lattice beams and an intensity of 0.1 $\mathrm{mW/cm^2}$ is sent along the Oz axis, two resonances are observed on the probe transmission spectrum [see Fig. 3(a) obtained for $\theta_x = \theta_y = 30°$]. The higher frequency component corresponds to the Ω_z vibration mode, whereas the second resonance is located near the position expected for the Ω_x vibrational mode. In fact, such a resonance was already obtained in [4], where it was attributed to a possible misalignment or intensity imbalance of the lattice beams. We thus carefully controlled the symmetry of the experimental setup, but still observed a resonance in Ω_x. Hence, we conclude that this resonance arises from the elementary propagating mode described in this Letter. (When the probe has the same linear polarization as the counterpropagating lattice beams, the experimental transmission spectra only display the Ω_z resonance. The disappearance of the Ω_S resonance when the probe polarization is rotated is a supplementary argument in support of this structure's not being associated with the vibrational motion of localized atoms. This absence of the Ω_S resonance is related to the fact that for this probe geometry, the pump-probe excitation along Oz essentially corresponds to a modulation of optical pumping between adjacent potential wells, which therefore strongly interferes with the propagating excitation mode along Ox. All these results are in good agreement with numerical simulations performed in this polarization geometry.) As the probe angle θ_p is progressively increased from zero, the probe transmission spectrum changes in agreement with the preceding discussion, as can be seen in Fig. 3(b) obtained for $\theta_p = 25°$. On the one hand, a stimulated Raman resonance located around Ω_x appears, which is actually narrower than the Ω_S resonance of Fig. 3(a). On the other hand, a resonance located at the position expected from Eq. (1) for the Ω_{S+} resonance is apparent on the spectra. We have also indicated on the figure the expected position for the Ω_{S-} resonance, which becomes practically unobservable as θ_p approaches θ_x. More generally, we have investigated these new resonances for various values of θ_x and θ_y in the range 15°–30°

and always found results in agreement with the preceding analysis [10]. We have also studied the positions of the Ω_{S+} and Ω_{S-} resonances versus θ_p. These positions are in excellent agreement with the predictions of Eq. (1) and with the results obtained from numerical simulations [9].

Finally, one can wonder whether a $J = 1/2 \rightarrow J' = 3/2$ atomic transition can reliably account for experiments performed with the $F = 4 \rightarrow F' = 5$ transition of cesium. There is indeed an obvious difference between both situations because, in contrast with the scheme of Fig. 1, the lowest adiabatic potential surface does not cross other potential curves in the $F = 4 \rightarrow F' = 5$ case. As a consequence, atomic propagation from a σ^+ to an adjacent σ^- well can proceed through adiabatic following of the same potential surface, without involving optical pumping processes. In fact, the adiabatic propagation scheme strictly applies for those atoms having a sufficiently small velocity in the vicinity of the maxima of the lowest potential curve. Atoms having larger velocities will undergo diabatic transfers toward higher potential surfaces, from which they will be optically pumped back toward the lowest potential wells, yielding a propagation scheme similar to the one described in this Letter.

In conclusion, we have identified a novel stimulated scattering process that shares some characteristics with recoil-induced resonances [11] and stimulated Brillouin scattering, which both rely on a spatial bunching mechanism. However, contrary to recoil-induced resonances, the present density modulation is intrinsically propagating and is characterized by a well-defined propagation velocity depending on the lattice geometry. We have reported the experimental observation of this novel stimulated scattering process, which should admit a spontaneous analog observable on the fluorescence [12] or the intensity correlation spectra [13] of a standard tetrahedron lattice.

The authors are grateful to C. Triché and C. Robilliard for stimulating discussions. This work was partly supported by the European Union and NEDO. Laboratoire Kastler-Brossel is an unité de recherche de l'Ecole Normale Supérieure et de l'Université Pierre et Marie Curie associée au CNRS.

*Permanent address: Institut d'Optique Théorique et Appliquée, BP 147, F-91403 Orsay cedex, France.
†Present address: Clarendon Laboratory, Magdalen College, Parks Road, Oxford 0X1 4AU, United Kingdom.

[1] See, for example, Y. R. Shen, *The Principles of Nonlinear Optics* (Wiley, New York, 1984); R. W. Boyd, *Nonlinear Optics* (Academic Press, New York, 1992).
[2] G. Grynberg *et al.*, Phys. Rev. Lett. **70**, 2249 (1993); A. Hemmerich, C. Zimmerman, and T. W. Hänsch, Europhys. Lett. **22**, 89 (1993); G. Birkl *et al.*, Phys. Rev. Lett. **75**, 2823 (1995).
[3] K. I. Petsas, A. B. Coates, and G. Grynberg, Phys. Rev. A **50**, 5173 (1994).
[4] P. Verkerk *et al.*, Europhys. Lett. **26**, 171 (1994).
[5] Y. Castin, J. Dalibard, and C. Cohen-Tannoudji, in *Light-Induced Kinetic Effects on Atoms, Ions and Molecules*, edited by L. Moi *et al.* (ETS Editrice, Pisa, 1991).
[6] This trajectory was computed from the three-dimensional optical potential by constraining the atomic motion along an x direction connecting the potential minima. Projections of two-dimensional atomic trajectories onto the x direction yield comparable results.
[7] M. Holland *et al.* (to be published); S. Marksteiner, K. Ellinger, and P. Zoller (to be published).
[8] This is because the Raman operator, which is proportional to the product of the pump and probe fields, is an *even* function of x and therefore cannot connect adjacent vibrational levels.
[9] J.-Y. Courtois, in Coherent and Collective Interactions of Particles and Radiation Beams, Proceedings of the International School of Physics "Enrico Fermi," Course CXXXI, edited by A. Aspect, W. Barletta, and R. Bonifacio (to be published).
[10] Our experimental setup did not permit us to study the range $30°-50°$ for the angles. We performed an experiment for $\theta_x = \theta_y = 55°$ and for $\theta_p = 0°$ and $20°$ and did not find a resonance of the Ω_{S+} or Ω_{S-} type. The absence of these resonance for large angles is also found in the numerical simulations and is associated with a stronger coupling between the motions along x and z.
[11] J. Guo *et al.*, Phys. Rev. A **46**, 1426 (1992); J.-Y. Courtois *et al.*, Phys. Rev. Lett. **72**, 3017 (1994).
[12] P. S. Jessen *et al.*, Phys. Rev. Lett. **69**, 49 (1992).
[13] C. Jurczak *et al.*, Opt. Commun. **115**, 480 (1995).